Theoretical study of the stability of beryllium oxide (110) and (001) surfaces in dense wurtzite and layered graphitic phases

A. Lichanot, I. Baraille, C. Larrieu, and M. Chaillet
Laboratoire de Chimie Structurale, Université de Pau et des Pays de l'Adour,
Unité de Recherche Associeé 474, Institut de Formation et de Recherche, Rue Jules Ferry, 64000 Pau, France
(Received 22 May 1995; revised manuscript received 11 September 1995)

The *ab initio* Hartree-Fock linear combination of atomic orbitals method implemented in the program CRYSTAL is used to study the relative stability of the dense wurtzite and layered graphite phases of beryllium oxide along the transformation pathway *wurtzite→graphite*. Bulk electronic structures are compared. Geometric and energetic relaxation of slabs parallel to the (110) and (001) surfaces of these two phases, respectively, are calculated in order to estimate the changes of the electronic structure, population analysis, electron charge densities, band structure, and density of states of the surface ions with respect to the bulk.

I. INTRODUCTION

It is well known that beryllium oxide BeO naturally occurs with a wurtzite-type structure. Calculations made from local-density-functional theory,[1] correlated with the *ab initio* LCAO (linear combination of atomic orbitals) Hartree-Fock approach[2,3] support this result when comparing the stability of the wurtzite and zinc-blende-type structures. Moreover, the Zunger-Cohen density-functional pseudopotential[4,5] applied to octet binary compounds leads to a partition of the structural map R_σ versus R_π (R are linear combinations of s and p valence radii) in six structure-type parts.[6] In this scheme, beryllium oxide is located at the boundary of the wurtzite, zinc-blende, and graphite parts, while the other beryllium chalcogenides are near the zinc-blende–graphite boundary. Finally, high-pressure and high-temperature effects on BeO also allow rocksalt[7] and tetragonal β-beryllia[8] structures, respectively.

It must be noted that the location of a BeO layered structure near the graphite boundary is in agreement with the existence of other isoelectronic compounds formed by first-row elements BN and C. In a recent work, Continenza, Wentzcovitch, and Freeman[9] have compared the stabilities of the dense wurtzite and layered graphitic phases. Their theoretical study was made with a local-density approximation (LDA) applied to the density-functional theory (DFT).[10] Their results, compared with the BN and C available ones, emphasize the unstable character of the graphitic phase which, up to now, has not been isolated from experiment. On the transition pathway chosen by these authors, the transformation energy *wurtzite→graphite* remains hypothetical, since the transition state has not been obtained.

The aim of this work is to calculate the electronic structure of beryllium oxide, and particularly the study of the (110) and (001) faces which play an important role in the binding of the bulk and which can bring fundamentals into the relative stability of the wurtzite and graphite phases. This work was performed with the *ab initio* restricted Hartree-Fock method using atomic all-electron basis sets. The transition pathway *wurtzite→graphite* corresponding to a less-motion path was calculated considering the variations of the geometric parameters a, c, and u of the hexagonal compact cell (u is the distance between the beryllium and oxygen planes) with the same symmetry $P_{6_3/mmc}$ (D^4_{6h}) along the transformation.

The (110) and (001) surfaces were more carefully investigated. Geometric structures and energies were calculated in their unrelaxed and relaxed states, and the electronic structures deduced. In this study, the semi-infinite crystal is built from a slab of atomic layers parallel to the chosen surface. This model,[11] already adopted for Li_2O (Ref. 12) and Li_2S (Ref. 13) compounds, leads to typical results for the surface properties when the slab thickness includes four atomic layers.

II. COMPARATIVE STUDY OF BeO WURTZITE AND BeO GRAPHITE BULK PROPERTIES

The compared stability of the wurtzite and zinc-blende phases of beryllium oxide and the wurtzite electronic structure were discussed in a previous paper,[3] within an *ab initio* LCAO Hartree-Fock (HF) self-consistent-field (SCF) scheme adjusted to the study of periodic systems[14] and implemented in the program CRYSTAL.[15] In the most stable wurtzite phase, we have chosen to study the (110) and (001) faces, which are rather different from a structural point of view among several reticular planes of great importance to explain the bulk binding of BeO. The first face can be easily described by a neutral two-dimensional cell having two molecular units BeO, while the second one must be described in a three-dimensional cell made of beryllium and oxygen parallel planes separated by the u distance. Taking into account the ionic character of the compound, this situation implies a dipole moment which makes this second face unstable. It is assumed that this (001) surface can either exist only with defects or foreign elements capable of stabilizing it, or evolve into another structural form. This form should be BN-type structure (graphite type). This assumption is

based on the surprising absence of the beryllium oxide in the isoelectronic series of the first-row elements (BN and C).

A. Physical properties of the graphite phase and transition energy *wurtzite → graphite*

Computational details and all-electron basis sets (5–11 G for beryllium and 8–411 G for oxygen) are the same as those already used for the study of the wurtzite phase.[3] The evaluation of the Coulomb and exchange series is done by adopting the following values of truncation tolerances $ITOL_1=ITOL_2=ITOL_3=5$, $ITOL_4=6$, and $ITOL_5=12$. These values indicate that the two centers integrals are disregarded or neglected whenever the overlap is smaller than 10^{-ITOL}. 28 independent k points in the irreducible first Brillouin zone are used to calculate the wave function: they correspond to the shrinking value $IS=6$. The chosen values of the parameters $ITOL$ and IS are a good compromise between reasonable computational times and a sufficient accuracy of the total energy. Moreover, we have also optimized the most external Gaussian functions in the graphite form. The obtained values ($\alpha_{Be}^{(G)}=0.602, \alpha_{O}^{(G)}=0.213$) are more diffuse than those of the wurtzite phase ($\alpha_{Be}^{(W)}=0.664$, $\alpha_{O}^{(W)}=0.230$) and indicate a larger electronic confinement in a volume about 1.4 times higher (Table I).

The simultaneous optimization of the lattice parameters (a,c) with respect to the cell energy is obtained by a gradient method (Newton-Raphton method). The calculation of the first and second derivatives of the energy versus a and c shows that the optimized wurtzite and graphite structures are stationary points with a small difference in energy (Table I, Fig. 1).

Calculations had been performed at two levels. We first give the results obtained from the Hartree-Fock approximation [E_0(HF)] and those taking into account the electronic correlation evaluated according to the Perdew[16] formalism [E_0(HF-P)]. Lattice parameters and formation energies $\Delta_f E_0$(HF) and $\Delta_f E_0$(HF-P) per unit primitive cell taking free ions as references are given in Table I for the two approximations. Examination of this table shows that the graphite phase is less stable with respect to wurtzite by 0.18 eV at the HF level, and by 0.46 eV when the electronic correlation effect is taken into account. As already noted by Causá and Zupan,[17] only correlation correction of the total energy obviously improves the agreement with experiment for which the value 1.4043 a.u. (3686.9 kJ mol^{-1}) for the BeO wurtzite formation energy is given. A fourfold coordination of ions and a higher density of the wurtzite structure explains this result in spite of similar features corresponding to the Be-O bond length and ionic characters of the two phases.

TABLE I. Lattice parameters a (Å), c (Å) and u (cell fraction), total energies E_0 and formation energies $\Delta_f E_0$ in a.u. obtained at the equilibrium for the wurtzite, layered graphite structures and saddle point (SP) along the transition pathway wurtzite→graphite. The symbols (HF) and (HF-P) correspond to the calculations at the Hartree-Fock level and corrected *a posteriori* by the electronic correlation deduced from the Perdew formula (Ref. 16), respectively.

	BeO (wurtzite)	BeO (graphite)	BeO (SP)
E_0 (HF)	−89.7023	−89.6958	−89.6949
$\Delta_f E_0$ (HF)	1.3439	1.3374	
E_0 (HF-P)	−90.1386	−90.1220	
$\Delta_f E_0$ (HF-P)	1.4242	1.4076	
a	2.690	2.655	2.680
c	4.338	5.998	5.053
u	0.3795	0.5000	0.4793

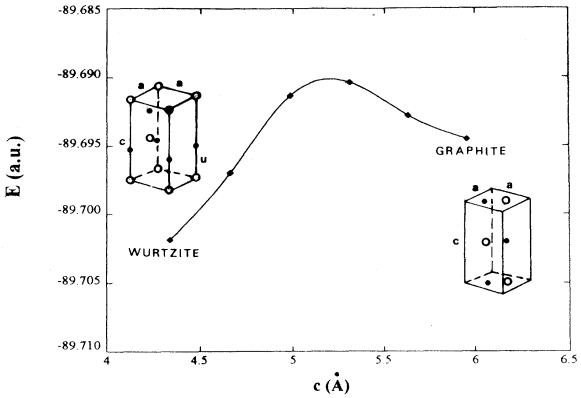

FIG. 1. Less-motion pathway going from wurtzite to graphite phases by maintaining the $P_{6_3/mmc}$ symmetry along the transformation.

Considering a less-motion pathway going from the wurtzite to the graphite phase by maintaining the $P_{6_3/mmc}$ symmetry along the transformation, a saddle point has been obtained by a simultaneous optimization of all geometric parameters on this path (Fig. 1). The lattice parameter c is the chosen transformation coordinate because it is the most sensitive to the *wurtzite→graphite* transition. All these calculations have been performed with the basis set optimized for the wurtzite. We have shown that the stationary points and their energetic characteristics are not sensitive to an optimization of the most external Gaussian functions of the basis set. Along the less-motion pathway the geometrical structure as a whole is slightly modified in a such manner that the *wurtzite→graphite* transition would be correctly treated. The transition state thus obtained is characterized by a sole negative second derivative of the energy with respect to the combination of the three geometrical parameters c, a, and u [these two last ones having a rather important contribution $(0.966c+0.202a+0.159u)$]. On the transformation pathway *wurtzite→graphite*, the energy value of the stationary point graphite is very close to the one corresponding to the saddle point (0.024 eV: 2.3 kJ mol^{-1}) (Table I and Fig. 1). This small value probably explains that the graphite layered phase cannot be stabilized and immediately turns into the wurtzite dense phase. The compared study of the wurtzite and graphite phases has been extended to the calculation of their electronic structure (Mulliken population analysis, band

structure, and electron charge density) as reported in the following.

B. Electronic structure: Mulliken analysis and band structure

The net charges on oxygen in the wurtzite and graphite phases are calculated from a Mulliken population analysis. It is well known that the use of Mulliken population is only an indication. The assignment of overlap populations is arbitrary, and the charge analysis roughly gives only an approximation of the electronic structure. Oxygen in BeO graphite has a smaller net charge by 0.075 e^- than oxygen in BeO wurtzite. This difference is only assignable to the populations of $p_{x,y}$ valence orbitals, which are 3.760 e^- in the graphite phase and 3.838 e^- in the wurtzite phase. This result indicates a less ionic character of the Be-O bond in the layered structure graphite, which is confirmed by the overlap population value between nearest neighbors (0.14 e^- in the graphite phase, 0.068 e^- in the wurtzite phase).

The band structure of the graphite phase is similar to the one of the wurtzite phase already published.[3] A few small but significant differences must be noted. The two first levels assigned to the pure 1s orbitals of oxygen and beryllium are more stable by about 0.8 eV in the BeO graphite phase than in wurtzite, while the reverse occurs for the energy corresponding to the lower part of the two following bands corresponding to the oxygen 2s and 2p orbitals, respectively. In the monoelectronic approximation, the energy location of the level corresponds to the energy necessary to extract one electron from the core state to infinity. Since the infinite Coulomb sums which lead to the position of the 1s core levels are similarly evaluated in the two structures, this small energy difference is only due to a geometry discrepancy where the Be-O bond (1.532 Å) shorter in the graphite phase than in the wurtzite one (1.646 Å) should account for this result. Moreover, the bandwidths associated with the 2s and 2p valence bands of oxygen are larger by 1.2 and 2.0 eV, respectively, in the wurtzite phase than in the graphite one. Taking into account the value of the O-O distances (2.658 Å in the graphite phase and 2.664 Å in wurtzite), the bandwidth of BeO graphite should be larger than that of the BeO wurtzite.[12] However, in this case, where these distances are very similar, the obtained result is explained both from a greater number neighbors O-O (12) in the dense phase and from its higher ionic character. Finally the oxygen p valence band of the two band structures graphite and wurtzite are not pure as in the fully ionic compounds: it has a 0.231e^- and 0.297e^- beryllium population in wurtzite and graphite phases, respectively. This last result expresses a slightly covalent character of the Be-O bond which is more important in graphite than in wurtzite structures, thus confirming the conclusions deduced from the Mulliken population analysis.

C. Electron charge density

Additional and more precise information about the comparison of the electronic structure of the graphite and wurtzite phases is obtained by examining total and difference electron charge-density maps. In particular, highly significant is the difference map which is obtained by subtracting from the total electron charge density the superposition of the isolated Be^{2+} and O^{2-} charge densities described with the same basis sets. For the graphite phase, Fig. 2 describes this map projected on a perpendicular plane to the [001] axis. It will be compared to the corresponding map of the wurtzite phase projected on a perpendicular plane to the [110] direction which better illustrates the bond structure.[3] An appreciable change of the isodensity curves around oxygen atoms shows a greater modification of the electron cloud in the graphite phase. This reflects both a larger contraction of this ion by the crystalline field effect and a more directional character of the Be-O bond in this phase. In the same way, a slight expansion of the Be^{2+} is observed, also confirmed by a Mulliken population analysis. The population of the more diffuse Gaussian function of the Be^{2+} basis set is 1.072 e^- in the graphite phase and therefore greater than in wurtzite (1.057 e^-) or than in the isolated ion (1.054 e^-). This additional result further supports a more covalent character of the Be-O bond in the layered phase.

III. STUDY OF [(110), WURTZITE] AND [(001), GRAPHITE] SURFACES: RELAXATION AND ELECTRONIC STRUCTURE

Several surface types (100), (110), and (001) associated with the wurtzite and graphite BeO structures could be studied, but we have chosen to turn our attention only to the (110) and (001) ones which are the most typical of the

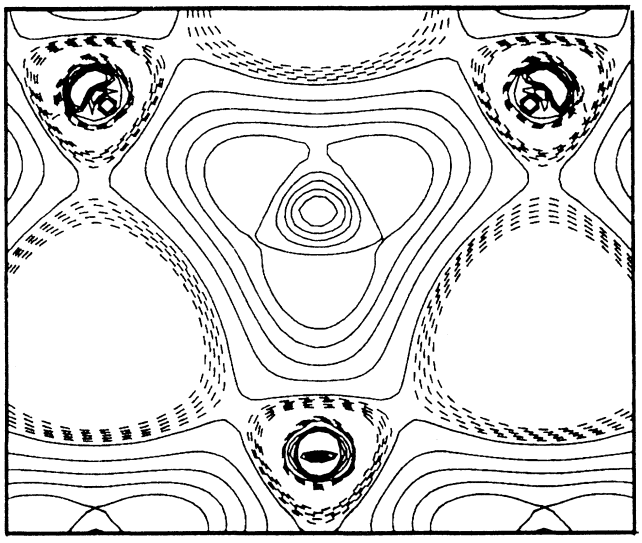

FIG. 2. Difference-electron charge-density map between the total-electron charge density of BeO graphite and the superimposition of free ions charge density described with the same basis sets. This map is projected on a plane perpendicular to the [001] direction. The step between two consecutive full lines (positive difference) is 0.01 a.u., and the step between two consecutive dashed lines (negative difference) is 0.002 a.u.

hexagonal structure. For previously mentioned reasons, it is assumed that the (001) surface of the dense phase moves toward the (001) surface of the layered phase; also, our study will be restricted to the (110) and (001) surfaces of the wurtzite and graphite phases, respectively, which are noted in the following [(110), wurtzite] and [(001), graphite].

Slab models parallel to the [(110), wurtzite] and [(001), graphite] surfaces including n repeat units are adopted and noted as S'_n and S_n ($2 \leq n \leq 4$), respectively. The geometric structure of the cell corresponding to each slab is built from the equilibrium lattice parameters of the bulk taken as reference. Thus the cell associated with the first slab is rectangular ($a\sqrt{3}, c$) with the P_{2_1ab} space group, while the cell associated with the second slab is hexagonal (a) with the P_{3m1} space group for odd n ($n=3$) and with the $P_{\bar{3}m1}$ space group for even n ($n=2$ and 4) [Figs. 3(a) and 3(b)]. The surface formation energy E^{sf} was calculated as half the difference between the slab energy per unit bidimensional cell (E_{s_n}) and the energy corresponding to the same number of bulk molecular units (E_0).

A. Geometric relaxation and surface formation energy

Each surface is composed of a neutral BeO layer, and the geometric parameters considered for the relaxation are d', d'', Δz, and Δx. They have been previously defined[12,13] and are represented in Figs. 3(a) and 3(b): their values are given in Table II. We have also reported in this table, for comparison, the relaxation parameters obtained from this same method for other similar oxide systems such as Li_2O (Ref. 18) and MgO,[19,20] which are cubic and highly ionic, or TiO_2,[21] which is tetragonal with a non-negligible covalent character. All these results are associated with slabs made of three or four layers.

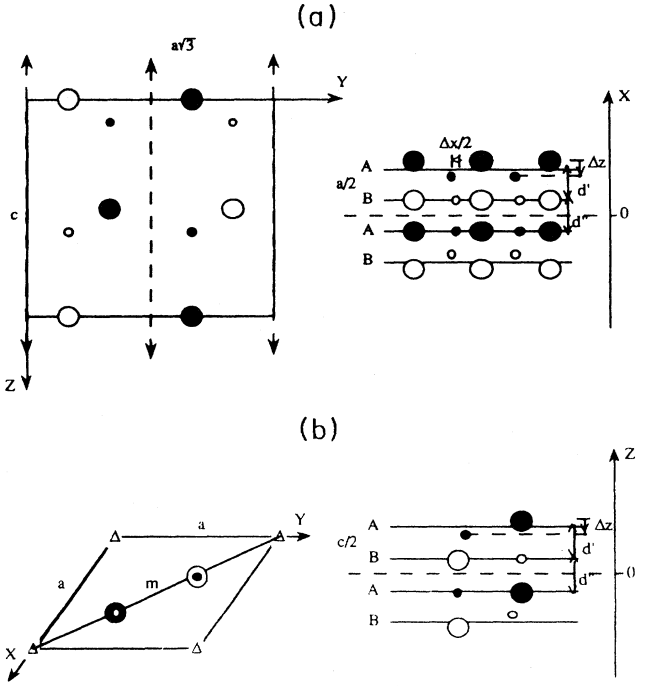

FIG. 3. Bidimensional cells and vertical sections of slabs made of four atomic layers. (a) Unit cell associated with the [(110), wurtzite] S'_n slab (P_{2_1ab}). (b) Unit cell associated with the [(001), graphite] S_n slab ($P_{\bar{3}m1}$). Beryllium and oxygen atoms are represented by small (o) and large (O) circles, respectively.

As in numerous studies made from the slab model,[18–22] the convergence of the surface formation energies and relaxation parameters corresponding to the BeO S'_n and S_n slabs occurs quickly and takes place for a slab composed of three or four layers. Examination of Table II shows that the (001) surface formation energy of the BeO graphite is very small: this result appears consistent, since the cut of this crystalline phase perpendicular to the

TABLE II. Surface formation energy E^{sf}(J m^{-2}) of the unrelaxed and relaxed slabs and geometric relaxation parameters (a.u.), in [(110), wurtzite] (S'_n) and in [(001), graphite] (S_n) slabs of different thickness. $\Delta d'$ and $\Delta d''$ represent the changes in the distance between first and second and second and third atomic layers, respectively. Δz is the rumpling in the surface layer and Δx is the movement parallel to the surface of ions in the surface layer.

		E^{sf} unrelaxed	E^{sf} relaxed	$\Delta d'$	$\Delta d''$	Δz	Δx
BeO	S'_2	2.92	2.26	−0.36 (−27%)		−0.18 (−13%)	0.52 (12%)
wurtzite	S'_4	2.99	2.59	−0.16 (−12%)	0.13 (10%)	−0.12 (−9%)	0.41 (10%)
BeO	S_2	0.06(4)	0.050	−0.37 (−12%)		−0.02 (3%)	
graphite	S_3	0.06(4)	0.06	−0.08 (−3%)		−0.01 (−1%)	
	S_4	0.06(4)	0.06	−0.08 (−3%)	−0.1(−3%)	−0.01 (−1%)	
Li_2O[a]	(110)	1.54	1.26	−6%	1%	5%	10%
MgO[b]	(001)	1.43	1.41	0%		−0.9%	
MgO[b]	(110)	3.63	3.27	−6.7%		−1.5%	
TiO_2[c]	(110)	2.97	2.02			−6.5%	−6%

[a]Reference 18.
[b]References 19 and 20.
[c]Reference 21.

c axis occurs without breaking the Be-O bond; the binding energy between the layers is of Van der Waals type. Similarly, the geometric relaxation parameters of these same systems S_n are small and, as a consequence, the relaxation energy defined by the difference between the surface formation energy of the unrelaxed and relaxed slabs is very low. This result indicates that the (001) surface of the BeO layered phase is very stable, and that the BeO graphite bulk can be considered from this point of view as an infinite slab. On the other hand, the surface formation energy calculated from S'_n slabs corresponds to the breaking of one tetrahedral chemical Be-O bond having a slightly covalent character: its value is rather large. The change of each geometric relaxation parameter is near 10% and, among these values, those corresponding to $\Delta d''$ and Δz which express the moving away of the second layer from the third one and of the oxygen outwards the slab, respectively, are abnormally high when they are compared to those associated with other similar systems (Li_2O and MgO). The relaxation energy which follows these modifications is large (0.4 $J\,m^{-2}$), and indicates that the stability of the (110) surface of BeO wurtzite is not very high since its geometry is significantly disturbed and the bond length BeO is reduced on an average by 0.037 Å (2.2%) with respect to the bulk.

Generally speaking, surface relaxation effects must be larger for a given compound when the distance between the nearest planes and the coordination of the surface ions are lower. Comparison of results obtained for (001) and (110) MgO surfaces (Table II) is instructive from this point of view since the distance is reduced by a factor $\sqrt{2}$ for the (110) surface with respect to the (001) one, and the sixfold-coordinated ions in the bulk become fivefold and fourfold coordinated in the (001) and (110) surfaces, respectively. In the same way, the results corresponding to the Li_2O and MgO (110) surfaces can be compared since these compounds are both fully ionic and are only attributable to the surface effects. In this case, the distance between layers is reduced by the ratio $[a_0(Li_2O)]/[a_0(MgO)]=1.1$, and the change of the oxygen coordination number is 2 [from 8 for the bulk to 6 for the (110) surface]. When chemical effects are superimposed on the electrostatic ones in partially covalent compounds BeO, TiO_2, and α-Al_2O_3, the surface relaxation effects are increased. Comparison of the results associated with the surfaces in which the change of the atomic coordination is the same, such as Li_2O and BeO wurtzite on the one hand, and (001) MgO and TiO_2 on the other, supports this conclusion. Finally it can be noted that for α-Al_2O_3 (0001) and (10$\bar{1}$0) (Ref. 22) slabs having a net dipole perpendicular to the surface, the surface effects appear still increased. These slabs are ended by a monoatomic layer made of aluminum or oxygen atoms, respectively. The surface formation energies (5.2 and 5.7 $J\,m^{-2}$) and the approach of the surface toward the underlying layer (0.4 and 0.2 Å) show the size of these parameters. However, the corresponding relaxation energies are surprisingly small and very different from those calculated by Tasker[23] in a semiclassical model.

TABLE III. Mulliken populations corresponding to the oxygen orbitals of the valence shell in S'_4 and S_4 relaxed slabs. Symbols O_I and O_{II} are attached to the surface and internal oxygens, respectively. Values in italics correspond to the *unrelaxed slabs.*

			s	$p_{x,y}$	p_z	total
BeO wurtzite	bulk		1.975	3.838	1.933	7.746
	S'_4	O_I	1.971	3.805	1.942	7.718
			1.977	*3.825*	*1.947*	*7.749*
		O_{II}	1.982	3.859	1.926	7.767
			1.981	*3.857*	*1.923*	*7.761*
BeO graphite	bulk		1.949	3.760	1.963	7.672
	S_4	O_I	1.950	3.760	1.963	7.673
			1.950	*3.760*	*1.962*	*7.672*
		O_{II}	1.952	3.762	1.962	7.676
			1.952	*3.760*	*1.961*	*7.673*

B. Electronic structure

Mulliken population analysis (Tables III and IV), electron charge densities (Fig. 4), and band structures (Figs. 5 and 6) of the thickest S'_4 and S_4 slabs in their relaxed and unrelaxed (values in italics) states have been calculated. Particular attention will be focused on the change of the electronic structure surface oxygen (O_I) with respect to that of the bulk or inside-slab oxygen (O_{II}).

TABLE IV. Atomic electron charge (C), dipole moment (D_z), and quadrupole moment (Q_z) (in a.u.) perpendicular to the surface. Symbols O_I and O_{II} are attached to the surface and internal oxygens, respectively. Values in italics correspond to the *unrelaxed slabs.*

		C		D_z		Q_z	
		O_I	O_{II}	O_I	O_{II}	O_I	O_{II}
BeO wurtzite	S'_2	9.722		0.004		−0.257	
		9.756		*−0.019*		*−0.227*	
	S'_4	9.718	9.767	−0.066	−0.024	−0.077	−0.160
		9.749	*9.761*	*−0.098*	*−0.074*	*−0.027*	*−0.167*
BeO graphite	S_2	9.673		0.009		−0.545	
		9.671		*0.003*		*−0.552*	
	S_4	9.673	9.676	0.011	0.000	−0.550	−0.562
		9.672	*9.673*	*0.004*	*0.000*	*−0.553*	*−0.568*

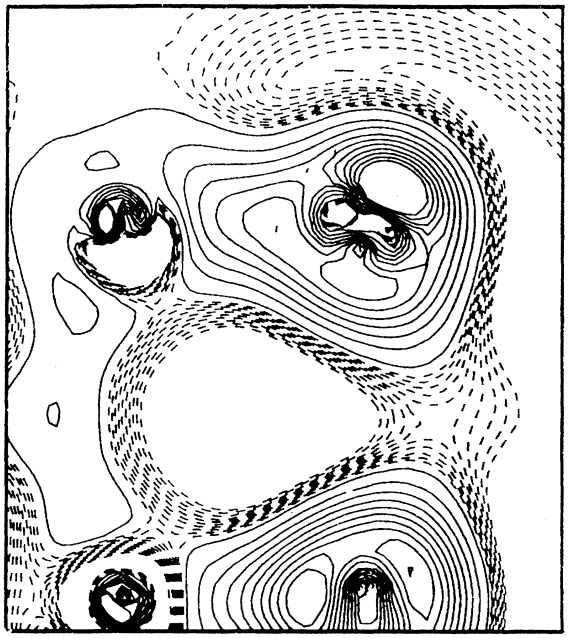

(a)

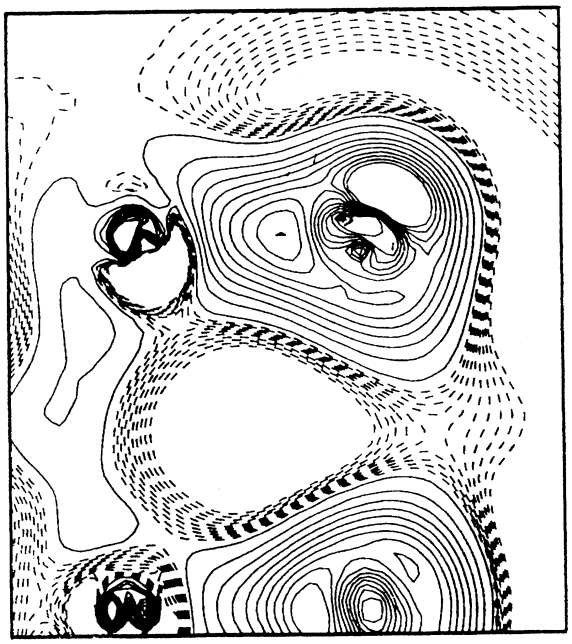

(b)

FIG. 4. Difference-electron charge-density map between the total-electron charge density of BeO wurtzite in the S_4' slab, and the superimposition of free ions charge density described with the same basis sets. This map is projected on the plane perpendicular to the [110] direction. The step between two consecutive full lines (positive difference) is 0.01 a.u. and the step between two consecutive dashed lines (negative difference) is 0.002 a.u. (a) and (b) correspond to unrelaxed and relaxed slabs, respectively.

Considering the S_4 *slab associated with the BeO graphite structure,* examination of Tables II and IV (giving the charges of the oxygen valence shells and the gross charges, the dipole and quadrupole moments of the oxygen charge distribution respectively owing to a Mulliken analysis) confirms the conclusions deduced from the energetics and relaxation considerations: the surface and relaxation effects do not practically disturb the geometry and the electronic structure of the surface atoms. However, a few comments must be made about the values of the multipole moments given in Table IV, in which the results corresponding to S_2 (and S_2') have been added for comparison. The atomic multipoles are defined by partitioning the electron charge distribution according to the Mulliken scheme. For a general shell (λ) the multipole moment $\gamma^{\lambda}(l,m)$ is defined by

$$\gamma^{\lambda}(l,m)=\sum_{\mu}\sum_{\nu}\sum_{g}P^{g}_{\mu\nu}\langle\chi^{0}_{\mu}|X^{m}_{l}|\chi^{g}_{\nu}\rangle \ ,$$

where χ^0_μ and χ^g_ν are the μth and the νth atomic orbitals centered in cells 0 and g, respectively, X_l^m is a spherical harmonic with (l,m) quantum numbers, and $P^g_{\mu\nu}$ is an element of the density matrix. In the present case, we have limited the calculations to the dipole (z; $l=1$, $m=0$) and quadrupole ($2z^2-x^2-y^2$; $l=2$, $m=0$) moments of the oxygen atom along the direction perpendicular to the surface of the slab, which thus measure the deformation of the oxygen electron cloud in the slab with respect to the situation of the bulk. Surface oxygens have a very small and positive dipole moment, three times larger in the relaxed slab than in the unrelaxed one. This corresponds to a displacement of the electron charge toward the inside of the slab, which is essentially due to the attraction of the beryllium nearest neighbors displaced out of the surface by the rumpling phenomenon. The smaller value observed in S_2 slab is due to the larger rumpling as shown in Table II. The negative value of the quadrupole component perpendicular to the slab reveals an elongation undergone by the electron cloud of the oxygen atom. Such a vertical elongation is related to the lateral Pauli repulsion between the electron distributions of adjacent beryllium and oxygen atoms. The absence of interaction between the layers of the structure explains that the Q_z value is practically the same for each layer of the slab. The removal of the beryllium oxygen in the surface layer following the rumpling lets us tentatively assume a smaller value for the surface in S_2 with respect to that of S_4 and the inner layers.

It is clear that such small deformations of the electron cloud cannot be observed, even on the difference electron charge-density map on S_n slab projected perpendicularly on the surface, which is the most accurate to show this deformation. Thus there is no difference between this map and the one corresponding to the bulk.

With respect to the band structure of the bulk discussed in Sec. II B for which the oxygen p-valence band projected on a surface perpendicular to the (001) direction is given in Fig. 6(a), the following main features corresponding to the S_4 slab can be underlined.

(i) A 0.2 eV stabilization of the lower part of the energy

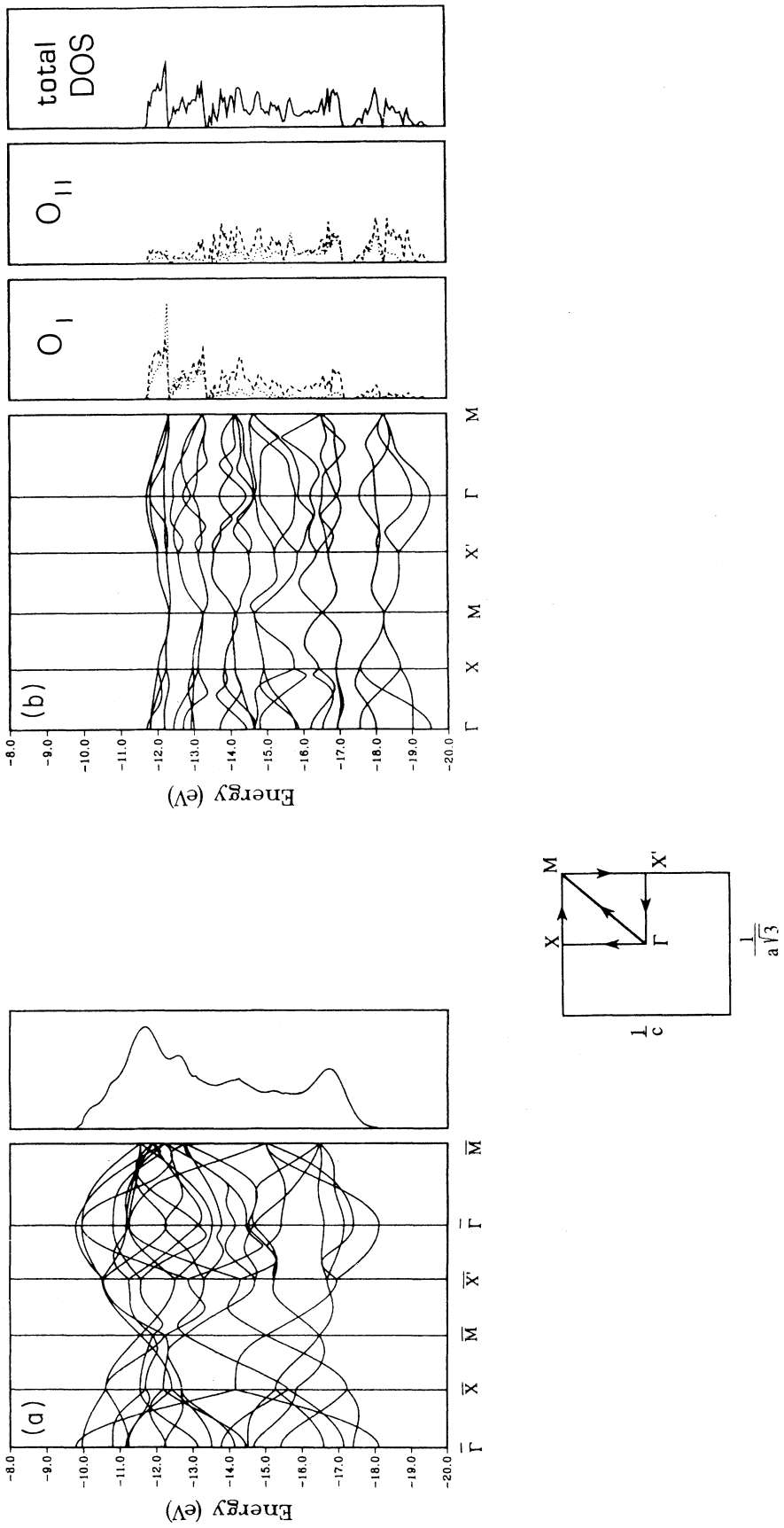

FIG. 5. Structure of the oxygen p-valence band and associated density of states (DOS). (a) Bulk. Projection of the band structure on a plane perpendicular to the [110] direction and the total DOS. (b) S_4' relaxed slab. Dashed and dotted lines represent the DOS's corresponding to the $p_{x,y}$ and p_z orbitals, respectively.

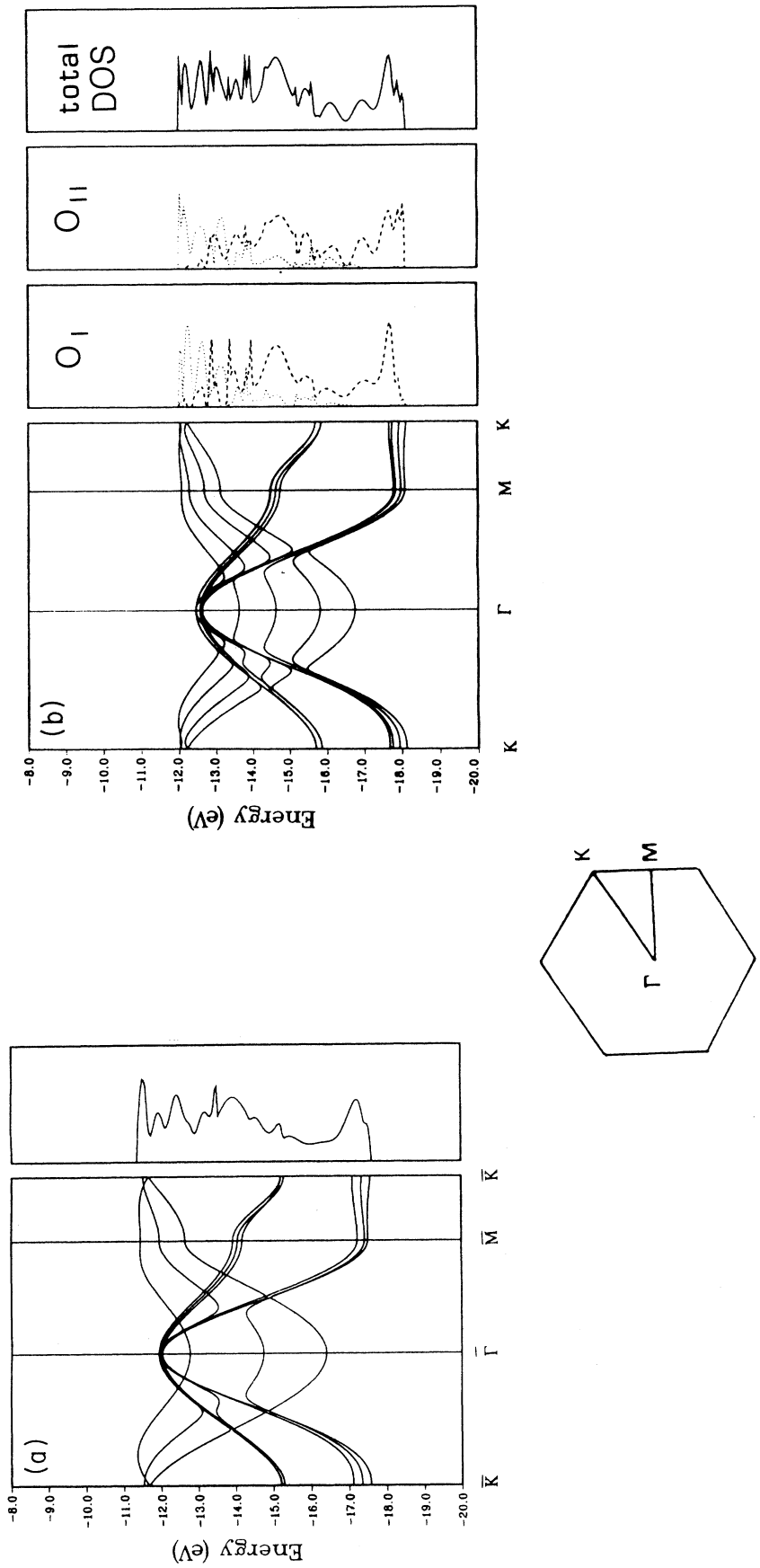

FIG. 6. Structure of the oxygen p-valence band and the associated density of states (DOS). (a) Bulk. Projection of the band structure on a plane perpendicular to the [001] direction and the total DOS. (b) S_4 relaxed slab. Dashed and dotted lines represent the densities of states corresponding to the $p_{x,y}$ and p_z orbitals, respectively.

bands occurs in the unrelaxed slab which is still increased by 0.3 eV when including the relaxation.

(ii) The oxygen valence bandwidth is slightly decreased (0.2 eV) in the unrelaxed slab by the loss of oxygen ions following the surface formation, then increased by 0.06 eV when taking into account the relaxation which approaches the surface oxygen toward those of the underlying layer by 0.036 Å.

Figure 6(b) represents the oxygen p-valence band in the S_4 slab along the path $K\Gamma MK$ of the first Brillouin zone with the densities of states (DOS's) associated with the $p_{x,y}$ (dashed line) and p_z (dotted line) orbitals of surface (O_I) and internal (O_{II}) oxygens. Figures 6(a) and 6(b) show that the band structures of the bulk BeO graphite and of the corresponding S_4 slab are the same, with the two small differences previously mentioned. The curves of the DOS's indicate that the p_z orbitals of surface and internal oxygen atoms have very pronounced maxima at the top of the band, while the $p_{x,y}$ orbitals are stabilized at the lower part of the band. This result clearly indicates that the reactivity of such a surface towards a gas phase will occur through the p_z oxygen orbitals.

Results for the *BeO wurtzite structure* (S'_n slabs) reported in Tables III and IV show that the surface and relaxation effects are much more significant than those calculated for the BeO graphite surface. In the unrelaxed slab, the ionic character of the Be-O bond is, on the whole, larger than in the bulk (Table III). This result, which specially affects the internal oxygen O_{II}, is rather surprising and proceeds from a new electronic breakdown between the $p_{x,y}$ or p_z orbitals. It must be noted that the breakdown is opposite for the surface and internal oxygens: the population of the $p_{x,y}$ orbitals of these last ones increases by 0.02 electron, while the population of the p_z orbital decreases by 0.01 electron with respect to the bulk reference. The effect of the geometric relaxation is only real for the surface oxygen (O_I), which becomes significantly less ionic owing to the decrease of the population of each valence orbital and $p_{x,y}$ orbital in particular. We find, with this result, a general and typical conclusion of the surface effect. Considering the dipole moments, their negative values remain low and indicate a small displacement of the electronic charge outward the slab as in the Li_2O case.[18] In the unrelaxed state, this result should probably be explained by the greater ionic character of the Be-O bond, which allows a more isotropic charge distribution around oxygen atoms which can be displaced outward from the slab by the loss of the crystal-field effect following the breaking of a Be-O bond. The more negative dipole moment of the oxygen atoms belonging to a thicker slab could be assigned to the amplification of this displacement by the repulsion between the oxygen electron cloud of two adjacent layers [Fig. 3(a)]. Geometric relaxation makes the dipole moments less negative. For the surface oxygens (O_I), the rumpling which has the same sign as in S_n (BeO graphite) and practically the same magnitude in S'_2 and S'_4 accounts for this result. For internal oxygen (O_{II}), it would be seen that the decrease of the repulsion in the inner part of the slab ($\Delta d'' > 0$) is practically the only factor acting on the O_{II} dipole moment, since the effects of $\Delta d'$ (<0) and Δz (<0) exactly complement each other. As in the S_n slabs of BeO graphite, the component Q_z of the oxygen quadrupole moment is negative, showing the vertical elongation of the oxygen electron cloud. In the unrelaxed S'_4 the Q_z value associated with the surface oxygen is abnormally low even if the presence of neighboring oxygens in the underlying layer makes the elongation less large. The smallest net charge on this oxygen further explains this value. Geometric relaxation which approaches the surface beryllium oxygen atoms by 0.034 Å increases the Pauli repulsion between their electron clouds, making the Q_z value more negative.

Previous main conclusions can be observed in Figs. 4(a) and 4(b), which represent difference-electron charge-density maps projected on a plane perpendicular to the (110) direction in the unrelaxed and relaxed S'_4 slabs, respectively. In particular, comparison of these figures clearly indicates the change of the surface Be-O bond toward a more covalent character when going from the unrelaxed slab to the relaxed one, while the internal Be-O bonds are not affected by the geometric relaxation. The vertical elongation of the oxygen (O_I and O_{II}) electron clouds are also well represented: the elongation for O_{II} is larger than the one for O_I. The slight elongation difference between the unrelaxed and relaxed slabs is also easily perceptible.

Comparison between the band structure and density of states associated with the valence orbitals corresponding to the bulk and the unrelaxed S'_4 slab will be studied, keeping in mind that the formation of the (110) surface is related to the cut of a tetrahedral Be-O bond. For a given ion, the number of opposite and the same kind of neighbors decreases, as deduced from a destabilization of the energy levels or bands associated with the surface ions and from a decrease of the corresponding bandwidth, respectively. These two phenomena act in reverse ways and practically compensate for each other in S'_4. Conversely, in the S'_2 slab, which has only surface ions, 1.3 and 1.6 eV destabilizations of the oxygen $2s$ and $2p$ orbitals, respectively, are observed, as well as a decrease by 1 and 2 eV of their bandwidths, owing to the change of the oxygen surroundings (from 12 to 6).

Geometric relaxation stabilizes in each case the energy of the lower part of the bands without modifying their bandwidth. This stabilization is rather large (1.4 eV for S'_2, 1.1 eV for S'_4). The size of the geometric relaxation explains this stabilization, while the difference between the two values corresponding to S'_2 and S'_4 is probably due to a greater value of $\Delta d'$ (27% in S'_2, 12% in S'_4). P valence bands of oxygen, and densities of states associated with the $p_{x,y}$ (dashed lines) and p_z (dotted lines) orbitals corresponding to the bulk projected on a plane perpendicular to the (110) direction and to O_I and O_{II} oxygens in the relaxed slab, are given in Figs. 5(a) and 5(b) for the path $\Gamma XMX'\Gamma M$ of the first Brillouin zone. It should be noted that the band structures of both unrelaxed and relaxed S'_4 slabs have the same shape; for this reason, only the last one is drawn. This structure is made of 24 bands corresponding to the eight oxygen atoms

present in the S_4' slab which are divided among four blocks. The most stabilized block is composed of four bands corresponding to the $p_{x,y}$ and p_z orbitals associated with the internal (O_{II}) oxygens as deduced from the DOS's curves. The middle block with 12 bands corresponds at once to the $p_{x,y}$ and p_z orbitals associated with the internal oxygens and with the $p_{x,y}$ of the surface (O_I) oxygens. Finally, the two upper blocks, which are separated from the central one by a 0.2 eV gap, are associated with a mixing of $p_{x,y}$ and p_z orbitals of the surface oxygens. Additional comments must be made when comparing the band structures of the oxygen p-valence band associated with the unrelaxed and relaxed slabs and bulk.

(i) The geometric relaxation effect shows only a stabilization of the unrelaxed structure, but does not modify the shape of its band structure in spite of the importance of the geometric relaxation parameters. This result is very different from the previous ones obtained for Li_2O,[18] for example.

(ii) The top of the p-valence band of oxygen is usually associated with the p_z orbital of the surface oxygens (Refs. 18 and 22 and BeO graphite) while in this case the $p_{x,y}$ orbitals must be also considered.

(iii) The shape of the band structure corresponding to the S_4' slab is rather different from the one corresponding to the bulk, including the same number of atomic layers which occurs in the form of a single manifold of 24 bands.

IV. DISCUSSION AND CONCLUSION

In order to more accurately understand the absence of a layered phase of the BeO compound in the isoelectronic series of the first-row elements (hexagonal boron nitride and graphite), a theoretical comparison of stabilities corresponding to the wurtzite and layered phases of beryllium oxide has been made. Our results confirm the experiment, showing that the layered phase is not observed, and also provides the reasons of this instability deduced from an analysis of a pathway simulating the transformation between dense and layered phases (wurtzite→graphite). Taking as a reference the study by Continenza, Wentzcovitch, and Freeman[9] based on the all-electron full-potential augmented-plane wave method, making use of the local-density approximation and using ideal geometry, our calculations clearly show that the BeO layered phase is clearly obtained as a stationary point of the potential hypersurface. The existence of a saddle point along the transformation pathway wurtzite→graphite near the graphite phase implies that the instability of this phase with respect to the wurtzite one is due to the very small barrier (23 kJ mol^{-1}) between the graphite phase and the saddle point. Compared physical properties of wurtzite and graphite phases show that BeO graphite is less stable with respect to the wurtzite one, and that their formation energy per unit primitive cell differs by 0.46 eV, of which 0.26 eV is assigned to the electronic correlation effect. A higher density of the wurtzite structure due both to a lesser volume and to a larger coordination of the ions explains these results on the whole. The Be-O bond in the graphite phase is shorter by 0.11 Å, and its ionic character is smaller than that of the wurtzite structure. This more covalent character is confirmed both by a more important deformation of the oxygen electron cloud in the electron charge-density maps, and by a larger participation of the beryllium to the population of the p oxygen valence band.

Slabs of sufficient thickness (four atomic layers) are studied in order to accurately obtain the geometry and the electronic structure of the surface ending them. In the case of S_n slabs parallel to the (001) face of the graphite structure, the surface formation energy, relaxation energy, and geometric relaxation parameters are very small. As a consequence, the electronic structure of the surface ions is practically not disturbed with respect to that of the bulk, and the stability of the (001) surface of the graphite phase can be considered as large. It thus represents a possible equilibrium structure corresponding to the transformation of the (001) wurtzite surface, unstable because of its dipole moment.

Conversely, all geometric relaxation parameters associated with a S_n' slab made of layers parallel to the (110) face of the wurtzite structure are rather large. Changes of around 10% in the distances between consecutive layers modification, of the rumpling and of the size of beryllium movement parallel to the surface indicate a nonnegligible rebuilding of this surface. As already observed in the study of numerous ionic compounds, the loss of one or several neighbors following the formation of a surface and its relaxation phenomenon slightly decrease the ionicity of the Be-O surface bond. Calculations of oxygen multipole moments and of electron charge densities show the vertical elongation of the electron cloud toward the exterior of the slab. With respect to the bulk properties the largest change is assignable to the band structure which seems rather different in the case of the S_n' slabs since it appears as four blocks separated by very small gaps. Relaxation does not allow us to join them into a single manifold as in the case of Li_2O.[18] Finally, we underline that the upper states of the oxygen p-valence band are occupied both by the $p_{x,y}$ and p_z orbitals, while for numerous other oxides and BeO graphite only the p_z orbitals take place. This difference must be kept in mind for the study of gas-phase chemisorption by these substrates, the accurate geometry and electronic structure of which are given in this study.

[1]K. J. Chang, S. Froyen, and M. L. Cohen, J. Phys. C **16**, 3475 (1983).

[2]J. C. Boettger, Ph.D. thesis, University of Illinois at Urbana, 1982.

[3]A. Lichanot, M. Chaillet, C. Larrieu, R. Dovesi, and C. Pisani, Chem. Phys. **164**, 383 (1992).

[4]A. Zunger and M. L. Cohen, Phys. Rev. B **18**, 5449 (1978).

[5]A. Zunger and M. L. Cohen, Phys. Rev. B **20**, 4082 (1979).

[6]M. L. Cohen, in *Structure and Bonding in Crystals,* edited by M. O'Keeffe and A. Navrotsky (Academic, New York, 1981),

Vol. I, p. 38.
[7]K. J. Chang and M. L. Cohen, Solid State Commun. **50**, 487 (1984).
[8]D. K. Smith, C. F. Cline, and S. B. Austerman, Acta Crystallogr. **18**, 393 (1965).
[9]A. Continenza, R. Wentzcovitch, and A. J. Freeman, Phys. Rev. B **41**, 3540 (1990).
[10]L. Hedin and B. I. Lundquist, J. Phys. C **4**, 2064 (1971).
[11]D. Vanderbilt and S. G. Lovie, Phys. Rev. B **30**, 6118 (1984).
[12]A. Lichanot, M. Gelize, C. Larrieu, and C. Pisani, J. Phys. Chem. Solids **52**, 1155 (1991).
[13]T. Ouazzani, A. Linchanot, C. Pisani, and C. Roetti, J. Phys. Chem. Solids **54**, 1603 (1993).
[14]C. Pisani, R. Dovesi, and C. Roetti, *Ab Initio Treatment of Crystalline Systems* (Springer-Verlag, Berlin, 1988).
[15]R. Dovesi, C. Pisani, C. Roetti, M. Causá, and V. R. Saunders, Computer Program CRYSTAL, Indiana University, Bloomington, IN, 1989; R. Dovesi, V. R. Saunders, and C. Roetti, CRYSTAL 92, User documentation, Gruppo di Chimica Teorica, University of Torino and SERC Daresbury Laboratory, 1992.
[16]J. P. Perdew and Y. Wang, Phys. Rev. B **45**, 13 244 (1991); J. P. Perdew, J. A. Chevary, S. H. Vosko, M. R. Pederson, D. J. Singh, C. Fiolhais, and Y. Wang, *ibid.* **46**, 6671 (1992).
[17]M. Causa and A. Zupan, Chem. Phys. Lett. **220**, 145 (1994).
[18]T. Ouazzani, A. Lichanot, and C. Pisani, J. Phys. Chem. Solids **56**, 915 (1995).
[19]M. Causa, R. Dovesi, C. Pisani, and C. Roetti, Surf. Sci. **175**, 551 (1986).
[20]M. Causa, R. Dovesi, E. Kotomin, and C. Pisani, J. Phys. C **20**, 4983 (1994).
[21]P. Reinhardt and B. A. Hess, Phys. Rev. B **50**, 12 015 (1994).
[22]C. Pisani, M. Causa, R. Dovesi, and C. Roetti, Prog. Surf. Sci. **25**, 119 (1987); M. Causa, R. Dovesi, C. Pisani, and C. Roetti, Surf. Sci. **215**, 259 (1989).
[23]P. W. Tasker, Adv. Ceram. **10**, 176 (1988).